Talanta 84 (2011) 324–329

Contents lists available at ScienceDirect

Talanta

journal homepage: www.elsevier.com/locate/talanta

Fluorescence detection of mercury(II) and lead(II) ions using aptamer/reporter conjugates

Yang-Wei Lin[a], Chi-Wei Liu[b], Huan-Tsung Chang[b,*]

[a] Department of Chemistry, National Changhua University of Education, Changhua, Taiwan, ROC
[b] Department of Chemistry, National Taiwan University, Taipei, Taiwan, ROC

ARTICLE INFO

Article history:
Received 22 October 2010
Received in revised form
21 December 2010
Accepted 7 January 2011
Available online 15 January 2011

Keywords:
Aptamer
Polythymine
Polyguanine
Mercury(II)
Lead(II)

ABSTRACT

We have developed a fluorescence technique for the detection of Hg^{2+} and Pb^{2+} ions using polythymine (T_{33})/benzothiazolium-4-quinolinium dimer derivative (TOTO-3) and polyguanine (G_{33})/terbium ions (Tb^{3+}) conjugates, respectively. Hg^{2+} ions induce T_{33} to form folded structures, leading to increased fluorescence of the T_{33}/TOTO-3 conjugates. Because Pb^{2+} ions compete with Tb^{3+} ions to form complexes with G_{33}, the extent of formation of the G_{33}–Tb^{3+} complexes decreases upon increasing the Pb^{2+} concentration, leading to decreased fluorescence at 545 nm when excited at 290 nm. To minimize interference from Hg^{2+} ions during the detection of Pb^{2+} ions, we conducted two-step fluorescence measurements; prior to addition of the G_{33}/Tb^{3+} probe, we recorded the fluorescence of a mixture of the T_{33}/TOTO-3 conjugates and Hg^{2+} ions. The fluorescence signal obtained was linear with respect to the Hg^{2+} concentration over the range 25.0–500 nM (R^2 = 0.99); for Pb^{2+} ions, it was linear over the range 3.0–50 nM (R^2 = 0.98). The limits of detection (at a signal-to-noise ratio of 3) for Hg^{2+} and Pb^{2+} ions were 10.0 and 1.0 nM, respectively. Relative to other techniques for the detection of Hg^{2+} and Pb^{2+} ions in soil and water samples, our present approach is simpler, faster, and more cost-effective.

1. Introduction

The monitoring of toxic metal ions, such as Hg^{2+} and Pb^{2+} ions, in aquatic ecosystems is necessary because they can have severe effects on human health and the environment [1,2]. The U.S. Environmental Protection Agency (EPA) permits the maximum level of mercury in drinking water to be 10 nM (2.0 $\mu g\,L^{-1}$) and considers the level of lead in the blood to be toxic when it is greater than or equal to 480 nM. The U.S. Food and Drug Administration suggests an action level for lead of 2.5 μM (518 $\mu g\,L^{-1}$) in products intended for children. In addition to the low concentrations of heavy metal ions, real samples are usually complicated by the presence of other ions, making the determination of Hg^{2+} and Pb^{2+} a difficult task. Although inductively coupled plasma mass spectrometry (ICP-MS) is a powerful tool for the determination of these two metal ions, commercially available ICP-MS systems are bulky and costly and require expensive gases; therefore, their use is limited for on-site analysis [3,4].

The last few years have witnessed great progress in the development of optical and electrochemical techniques for the detection of metal ions [5–14]. Nevertheless, many of these systems have limited practical use because of, for example, poor aqueous solubility, cross-sensitivity toward other metal ions, matrix interference, high cost (e.g., enzymes), complicated processing, the use of unstable molecules, and/or poor sensitivity. Recently, detection systems using DNA have become popular for the detection of metal ions, mainly because DNA is stable, highly soluble in aqueous solution, and a specific binder of certain metal ions, including K^+, Hg^{2+}, and Pb^{2+} ions [15–19]. Aptamers (single-stranded DNA or RNA) that act in a manner similar to that of antibodies in their recognition of target metal ions are also interesting sensing systems [20,21]. The so-called "systematic evolution of ligands by exponential enrichment" (SELEX) is a practical process for the isolation of aptamers. The advantages of using aptamers over antibodies include their high stability, relatively simple synthesis, ready structural modification, and high affinity toward metal ions. Fluorescence resonance energy transfer (FRET)-based DNAzyme systems have been demonstrated for the sensing of Pb^{2+} ions [22–25]. In the presence of Pb^{2+}, the DNAzyme catalyzes the hydrolytic cleavage of a substrate, thereby turning on the fluorescence for sensing. In addition, DNA-functionalized gold nanoparticles (Au NPs) have become interesting species for the detection of metal ions, including Hg^{2+}, Pb^{2+}, and $UO_2{}^{2+}$ ions [26–30]. By taking advantage of the high molar extinction coefficients and superior quenching capability of Au NPs, DNA-Au NP sensing systems can readily detect metal ions at the nanomolar level. Although these DNA-based detection systems are

* Corresponding author at: Department of Chemistry, National Taiwan University, 1, Section 4, Roosevelt Road, Taipei 106, Taiwan, ROC.
Tel.: +886 2 33661171; fax: +886 2 33661171.
E-mail address: changht@ntu.edu.tw (H.-T. Chang).

0039-9140/$ – see front matter © 2011 Elsevier B.V. All rights reserved.
doi:10.1016/j.talanta.2011.01.016

highly selective and sensitive for metal ions, all previous examples have been designed for the sensing of only a single type of metal ion. Recently, a thrombin-binding aptamer (TBA) labelled with the fluorophore carboxyfluorescein (FAM) and the quencher 4-([4-(dimethylamino)phenyl]azo)benzoic acid (DABCYL) at its 5′ and 3′ termini, respectively, has been used for the highly selective and sensitive detection of Hg^{2+} and Pb^{2+} ions, with limits of detection (LODs) of 5.0 nM and 300 pM, respectively [16]. Although this performance is impressive, conjugation of the fluorophore and quencher to the TBA is necessary and masking agents (phytic acid and a random DNA/NaCN mixture) are required to reduce matrix interference.

In this paper, we present a technique for the highly selective and sensitive detection of Hg^{2+} and Pb^{2+} ions using two non-fluorescent DNA sequences—polythymine (T_{33}) and polyguanine (G_{33})—and two reporters—benzothiazolium-4-quinolinium dimer derivative (TOTO-3) and terbium ions (Tb^{3+}). The T_{33} and G_{33} strands form complexes separately with Hg^{2+} and Pb^{2+} ions through T–Hg^{2+}–T and Pb^{2+}–G-quartet coordination, respectively, leading to increased and decreased fluorescence, respectively. We investigated the roles of the pH, temperature, the length and sequence of the probe, the probe-to-reporter ratio, and the order of addition of the probes in determining the sensitivity and specificity for the two metal ions. The practicality of the present assay was validated by the analysis of soil and pond water samples.

2. Experimental

2.1. Chemicals

Tris(hydroxymethyl)aminomethane (Tris), acetic acid, and all of the metal salts used in this study were purchased from Aldrich (Milwaukee, WI). TOTO-3 was obtained from Molecular Probes (Portland, OR). DNA samples (G_7, G_{15}, G_{33}, G_{50}, T_{33}, A_{33}, and C_{33}) were purchased from Integrated DNA Technology (Coralville, IA). Montana soil (SRM 2710) was obtained from the National Institute of Standards and Technology (NIST, MD). Milli-Q ultrapure water was used in each experiment.

2.2. T_{33}/TOTO-3 and G_{33}/Tb^{3+} conjugates for the detection of Hg^{2+} and Pb^{2+} ions

Stock solutions of TOTO-3 (0.2 μM) and Tb^{3+} (1.0 μM) were prepared in Milli-Q ultrapure water. Aliquots of the TOTO-3 solution (40 μL) were added separately to 10 mM Tris-acetate (pH 7.4) solutions containing Hg^{2+} (0–10 μM), Pb^{2+} (0–10 μM), and T_{33} (10 nM) to give final volumes of 400 μL. After equilibration at ambient temperature for 15 min, the fluorescence intensities at 660 nm of the mixtures were measured using a Cary Eclipse fluorescence spectrophotometer (Varian, CA), with excitation at 620 nm for the detection of Hg^{2+} ions. Aliquots of G_{33} (100 nM, 50 μL) were then added to the mixtures. After equilibration for 10 min, aliquots of Tb^{3+} ion (1.0 μM, 50 μL) were added. The final concentrations of G_{33} and Tb^{3+} were 10 and 100 nM, respectively. After equilibration for 20 min, the fluorescence at 545 nm was recorded to determine the concentration of Pb^{2+} ions, with excitation at 290 nm. For control experiments, the same analytical processes were applied, except that, instead of G_{33} being used, T_{33}, A_{33}, or C_{33} was added to the mixtures.

2.3. Analysis of real samples

Acidic digestion of soil samples (1.00 g) was performed according to EPA Method 305B [31]. Aliquots (50 μL) of the soil samples (0.25×) were spiked with standard solutions of Hg^{2+} over the concentration range 10–100 nM. For determining the concentration of Hg^{2+} ions, the mixtures were then diluted to 500 μL with 10 mM Tris-acetate solution (pH 7.4) containing the T_{33} (10 nM) and TOTO-3 (20 nM). After fluorescence measurement, aliquots (2 μL) of the mixtures were spiked with standard solutions of Pb^{2+} over the concentration range 5.0–50 nM. The G_{33} (10 nM) and Tb^{3+} ions (100 nM) were added to the mixtures in the sequence outlined above for the standard sample, and the spiked samples were then further diluted to 500 μL with 10 mM Tris-acetate solution (pH 7.4) prior to detection of the Pb^{2+} ions.

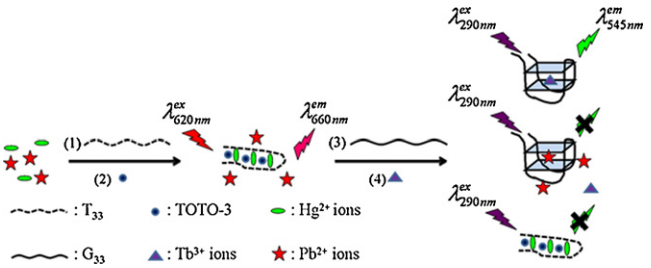

Scheme 1. Cartoon representation of the sensing strategy of using the T_{33}/TOTO-3 and G_{33}/Tb^{3+} conjugates for the detection of Hg^{2+} and Pb^{2+} ions, respectively.

A water sample collected from a pond on the campus was filtered through a 0.2 μM membrane. Aliquots of the pond water (250 μL) were spiked with standard solutions (50 μL) containing Hg^{2+} ions at concentrations over the range 25–250 nM. The spiked samples were then diluted to 500 μL with 10 mM Tris-acetate solution (pH 7.4) containing the T_{33} (10 nM) and TOTO-3 (20 nM). After fluorescence measurement, the mixtures were spiked with standard solutions of Pb^{2+} over the concentration range 5.0–50 nM. For the determination of Pb^{2+} ions, the G_{33} (10 nM) and Tb^{3+} ions (100 nM) were added sequentially to the mixtures described above for the standard sample.

3. Results and discussion

3.1. Sensing strategy

Scheme 1 displays our strategy for the detection of Hg^{2+} and Pb^{2+} ions using the T_{33}/TOTO-3 and G_{33}/Tb^{3+} conjugates, respectively. This detection system features two components: (i) a Hg^{2+}-induced fluorescence increase for the T_{33}/TOTO-3 conjugates and (ii) competition between Pb^{2+} and Tb^{3+} ions to form complexes with G_{33} and, thereby, decrease the fluorescence of the G_{33}/Tb^{3+} conjugates. In the absence of Hg^{2+} ions, T_{33} exists in aqueous solution with a random-coil structure. Because the interactions between the randomly coiled T_{33} and TOTO-3 are weak, the fluorescence of such a mixture is weak. Once T_{33} interacts with Hg^{2+} ions through T–Hg^{2+}–T coordination, its structure changes to a folded conformation [18,28,32,33]. In our previous study, we determined the binding constant (K_b) for the T_{33}/Hg^{2+} conjugates to be $6.1 \times 10^6\ M^{-1}$ using a Scatchard plot [18]. Hg^{2+} specifically bound with the T:T mismatched based pair at a molar ratio of 1:1 with K_b of ca. $10^6\ M^{-1}$ had been determined by conducting isothermal titration calorimetry (ITC) [34,35]. As a result, greater amounts of TOTO-3 become intercalated with T_{33}. As a result of reduced collisions and the forming of stiffer structures, the Hg^{2+}–DNA–TOTO-3 complexes fluoresce more strongly than does free TOTO-3. The C_{33}, G_{33}, and A_{33} strands do not form strong complexes with Hg^{2+} ions [18,28,36]. On the other hand, G_{33} also exists in a random-coil structure in aqueous solution. Upon binding with Tb^{3+} ions through cooperative coordination of nitrogen and oxygen atom donors from base and phosphate groups, G_{33} changes its structure to a G-quartet structure. As a result of efficient energy transfer from nucleobases to the Tb^{3+} ions and the loss of hydration water molecules (thereby

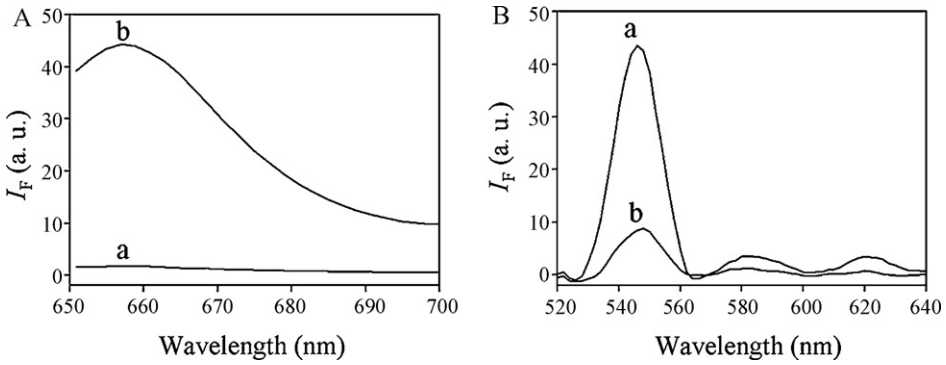

Fig. 1. Fluorescence spectra of (A) the T_{33} (10 nM) and TOTO-3 (20 nM) in the (a) absence and (b) presence of Hg^{2+} (500 nM) in 10 mM Tris-acetate (pH 7.4) and (B) the G_{33} (10 nM) and Tb^{3+} (100 nM) in the (a) absence and (b) presence of Pb^{2+} (500 nM) in 10 mM Tris-acetate (pH 7.4) containing Hg^{2+} (100 nM) and the T_{33}/TOTO-3 conjugates. Excitation wavelengths: (A) 620 and (B) 290 nm. Fluorescence intensities (I_F) are plotted in arbitrary units (a. u.).

reducing the yield of deactivation process through O–H vibrational manifold), the fluorescence of Tb^{3+} increases [37–41]. Comparing the A_{33}, T_{33}, and C_{33} probes, only the G_{33}/Tb^{3+} conjugates provided strong fluorescence. Because Pb^{2+} and Tb^{3+} ions interact competitively with G_{33} to form G-quadruplexes [42,43], decreased amounts of G_{33}/Tb^{3+} conjugates formed upon increasing the concentration of Pb^{2+}, leading to decreased fluorescence. Notably, the strength of the G_{33}/Pb^{2+} conjugates (K_b = ca. 10^7 M^{-1}) is greater than that of the G_{33}/Tb^{3+} conjugates (K_b = ca. 10^6 M^{-1}) [44]. Since Hg^{2+} ions but not T_{33}–Hg^{2+} complexes competed with Tb^{3+} ions to form G-quadruplexes with G_{33}, the T_{33}/TOTO-3 conjugates was added to detect Hg^{2+} ions before detection of Pb^{2+} ions using the G_{33}/Tb^{3+} conjugates.

We performed proof-of-concept experiments for the detection of Hg^{2+} and Pb^{2+} ions using the T_{33}/TOTO-3 and G_{33}/Tb^{3+} conjugates. Curve a in Fig. 1A reveals that the fluorescence of TOTO-3 (20 nM) at 660 nm in the presence of 10 nM T_{33} is very weak when excited at 620 nm, consistent with the weak interactions expected between TOTO-3 and the random-coil T_{33}. After adding TOTO-3 to the mixture of Hg^{2+} ions (500 nM) and T_{33}, a rapid (<10 s) and significant (26.8-fold) increase in fluorescence intensity occurred (curve b in Fig. 1A). In the absence of T_{33}, we did not observe any change in the fluorescence spectrum of TOTO-3 (20 nM) after adding Hg^{2+} (500 nM). Curve a in Fig. 1B displays the fluorescence spectrum of Tb^{3+} ions (100 nM) bound to quadruplexes of G_{33} (10 nM) when excited at 290 nm; a maximum emission wavelength appears at 545 nm [38]. We detected no fluorescence in the absence of either G_{33} or Tb^{3+} ions. After sequentially adding G_{33} and Tb^{3+} ions to a mixture (pH 7.4) of Hg^{2+} ions (100 nM), Pb^{2+} ions (500 nM), and the T_{33}/TOTO-3 conjugates, we observed a notable (5.29-fold) decrease in the fluorescence of Tb^{3+} ions (curve b in Fig. 1B).

Next, we separately investigated the kinetics of forming folded structure of the G_{33} strand in the presence of Tb^{3+} and Pb^{2+} ions. The fluorescence intensity of the G_{33}/Tb^{3+} conjugates took 20 min to reach equilibrium. Its fluorescence decreased immediately once Pb^{2+} ions was added (Fig. 2A). Curve a in Fig. 2B shows the circular dichroism (CD) spectrum of the G_{33} in the absence of Tb^{3+} and Pb^{2+} ions, respectively. A negative band at 240 nm and a positive band at around 285 nm appeared, typically observed for the G_{33} probe with a random structure [44]. The addition of Tb^{3+} or Pb^{2+} ions caused significant changes in the CD spectrum (curves b and c in Fig. 2B); two new positive peaks at 240 nm and 310 nm and a negative peak at 265 nm appeared, revealing the formation of G-quadruplex structure [16,44].

3.2. Stability of G_{33}–Tb^{3+} conjugates

The broad excitation band centered at 250 nm corresponds to the absorption spectrum of G_{33}, indicating that the fluorescence of Tb^{3+} ions was sensitized as a result of energy transfer from the G-quadruplex. Thus, we investigated the effect of the concentration of G_{33} on the fluorescence in the presence of Tb^{3+} ions (100 nM) in 10 mM Tris-acetate solution (pH 7.4), revealing that the fluorescence intensity of the G_{33}/Tb^{3+} complexes increased upon increasing the G_{33} concentration up to 10 nM (Fig. 3A) and then decreased. By using a Scatchard plot, we calculated the K_b of G_{33}/Tb^{3+} conjugates to be 10^6 M^{-1}, with a stoichiometry coefficient (n) of 10 [45]. The K_b value agrees well with those for DNA, RNA and GMP complexes with Tb^{3+} [38,39]. We also investigated the role that the length of the polyguanine strand (G_7, G_{15}, G_{33}, G_{50}) played in determining the fluorescence of the DNA–Tb^{3+} complexes (Fig. 3B). The G_7/Tb^{3+} conjugates fluoresced weakly (only 7.1 × 10^{-3}

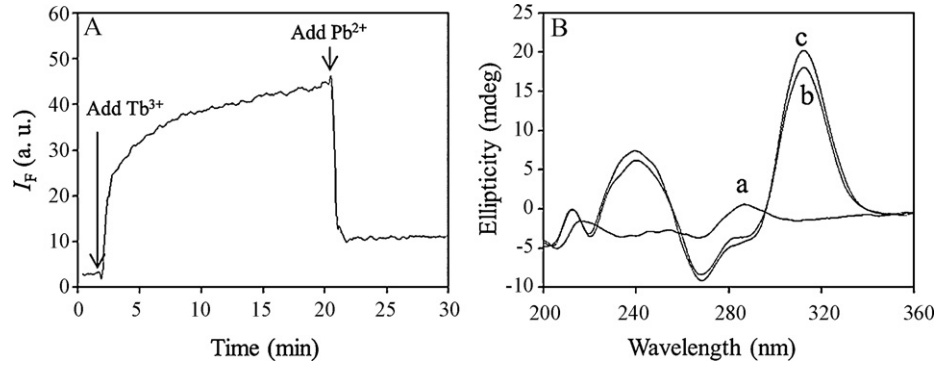

Fig. 2. (A) The folded kinetics of the G_{33} (10 nM) in 10 mM Tris-acetate (pH 7.4) containing Hg^{2+} (100 nM) in the presence of Tb^{3+} (100 nM) and Pb^{2+} (500 nM), respectively. (B) CD spectra of G_{33} (5.0 μM) in the (a) absence and the presence of (b) Tb^{3+} (50.0 μM) and (c) Pb^{2+} (50.0 μM), respectively. Other conditions were the same as those described in Fig. 1.

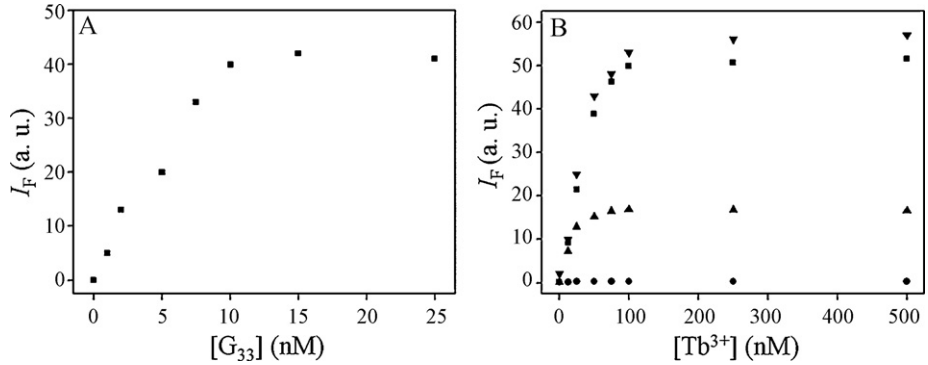

Fig. 3. Fluorescence of (A) G_{33}/Tb^{3+} conjugates plotted with respect to the concentration of G_{33} and (B) polyguanine/Tb^{3+} conjugates (▼, G_{50}; ■, G_{33}; ▲, G_{15}; ● G_7) plotted with respect to the concentration of Tb^{3+} ions. Concentrations of (A) Tb^{3+}: 100 nM, (B) polyguanine: 10 nM. Other conditions were the same as those described in Fig. 1.

times that of the G_{33}/Tb^{3+} conjugates), mainly because of their weak interactions (G-quadruplex structures were not formed). We found that the polyguanine required at least 15 bases to obtain a significant positive response (>50 times that of the G_7/Tb^{3+} conjugates). Although the fluorescence intensities of the Tb^{3+} complexes with polyguanines possessing more than 33 bases were slightly higher than that of the G_{33}/Tb^{3+} conjugates, their use was impractical, mainly because of their relatively high costs and lower purity.

Because environment factors such as pH of buffer solution and temperature affect the stability of the G_{33}/Tb^{3+} conjugates, the fluorescence of the G_{33}/Tb^{3+} conjugates under various conditions were investigated. The fluorescence intensity of the G_{33}/Tb^{3+} conjugates reached maximum at pH 7.4. At higher pH values, competition of OH^- with G_{33} to interact with Tb^{3+} ions became greater, leading to decreased fluorescence (Fig. S1A). On the other hand, at low pH values, the interaction between G_{33} and Tb^{3+} ions was weaker as a result of protonation of nitrogen on the bases. The fluorescence intensity of the G_{33}/Tb^{3+} conjugates decreased (50%) upon increasing the temperature from 20 to 70 °C (Fig. S1B), mainly because of G_{33} tend to form random structure to a greater degree (more rigid G-quadruplex structures become more unstable at higher temperature). The optimal conditions with respect to selectivity and sensitivity for this study were use of 10 nM G_{33} in 10 mM Tris-acetate buffer (pH 7.4) containing 100 nM Tb^{3+} ions and the analysis was conducted at room temperature.

3.3. Selectivity

We carefully tested the detection of Hg^{2+} and Pb^{2+} ions using the T_{33}/TOTO-3 and G_{33}/Tb^{3+} conjugates in four different buffer systems (10 mM, pH 7.4), including Tris-acetate, sodium acetate, sodium phosphate and sodium tetraborate. The values of $[(I_F - I_{F0})/I_{F0}]$ for the solutions buffered with Tris-acetate, sodium acetate, sodium phosphate and sodium tetraborate at 500 nM Hg^{2+} using the T_{33}/TOTO-3 conjugates were 10.7, 10.1, 3.20, and 2.81, respectively. Herein, I_F and I_{F0} represent fluorescence intensity in the presence and absence of the metal ion, respectively. Their values for 500 nM Pb^{2+} using the G_{33}/Tb^{3+} conjugates were 0.65, 0.62, 0.45, and 0.12, respectively. The sensitivity decreased upon increasing the stability of metal–anion complexes; for example, we obtained lower sensitivity for Pb^{2+} ions in phosphate buffer than that in Tris-acetate buffer (formation constants: $\log K_f = 43.5$ for Pb_3L_2 (L, phosphate) and $\log K_f = 4.1$ for PbL_2 (L, acetate)). We also tested the effect of buffer concentration on the detection of Hg^{2+} and Pb^{2+} using the T_{33}/TOTO-3 and G_{33}/Tb^{3+} conjugates in Tris-acetate buffer systems (pH 7.4). The values of $[(I_F - I_{F0})/I_{F0}]$ for Tris-acetate buffer systems with concentration of 10, 25, 50 and 100 mM at 500 nM Hg^{2+} ions using the T_{33}/TOTO-3 conjugates were 10.7, 5.4, 3.5, and 1.1, respectively. Their values for 500 nM Pb^{2+} ions using the G_{33}/Tb^{3+} conjugates were 0.65, 0.32, 0.22, and 0.13, respectively, mainly because of the formation of more stable metal–anion complexes upon increasing the buffer concentration ($\log K_f = 9.3$ for HgL_2 and $\log K_f = 4.1$ for PbL_2 (L, acetate)), leading to suppression of their interactions with the T_{33}/TOTO-3 and G_{33}/Tb^{3+} conjugates, respectively. The optimal conditions with respect to selectivity and sensitivity for this study were use of 10 mM Tris-acetate buffer (pH 7.4) at room temperature.

In a previous study, we found that the T_{33}/TOTO-3 conjugate is highly selective and sensitive for the detection of Hg^{2+} ions [18]. Indeed, its selectivity for Hg^{2+} over 18 other tested metal ions (Li^+, Na^+, K^+, Mg^{2+}, Ca^{2+}, Sr^{2+}, Fe^{2+}, Fe^{3+}, Al^{3+}, Cr^{3+}, Co^{2+}, Ni^{2+}, Cu^{2+}, Zn^{2+}, Pb^{2+}, Cd^{2+}, Ag^+, Au^{3+}; each 1.0 μM) was at least 265-fold [18]. Notably, the selectivity of T_{33} toward Hg^{2+} ions over Pb^{2+} ions was greater than 195-fold, revealing that Pb^{2+} ions were unlikely to interfere with the determination of Hg^{2+} ions. The nature of anions in mercury compounds (such as $Hg(ClO_4)_2$, $HgCl_2$ and $Hg(NO_3)_2$) did not play major roles in the detection of Hg^{2+} ions. To determine the selectivity of the G_{33}/Tb^{3+} conjugates toward Pb^{2+} ions, we also added Na^+, K^+, NH_4^+, Sr^{2+}, Pb^{2+}, Hg^{2+}, Pd^{2+}, Zn^{2+}, Ni^{2+}, Mn^{2+}, Cd^{2+}, Fe^{2+}, Co^{2+}, Cu^{2+}, Cr^{3+}, and Mg^{2+} ions (100 nM) separately into probe solutions containing Tb^{3+} and G_{33}. Only the presence of Pb^{2+} ions (100 nM) caused a decrease in the fluorescence of Tb^{3+} ions, revealing that G_{33} is selective for Pb^{2+} ions. Although K^+ ions stabilized the G-quadruplex structure, their stability with G quartets is much

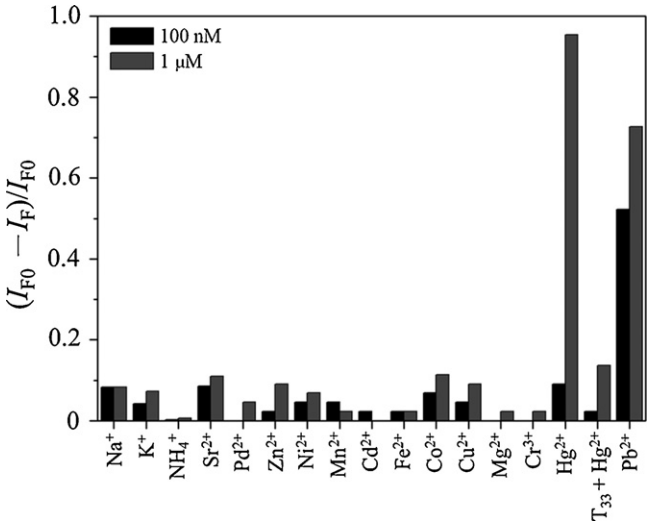

Fig. 4. Relative fluorescence intensity $(I_{F0} - I_F)/I_{F0}$ of the G_{33}/Tb^{3+} conjugates at 545 nm in the presence of metal ions (100 nM and 1.0 μM). I_F and I_{F0} represent fluorescence intensities in the presence and absence, respectively, of the metal ion. Other conditions were the same as those described in Fig. 1.

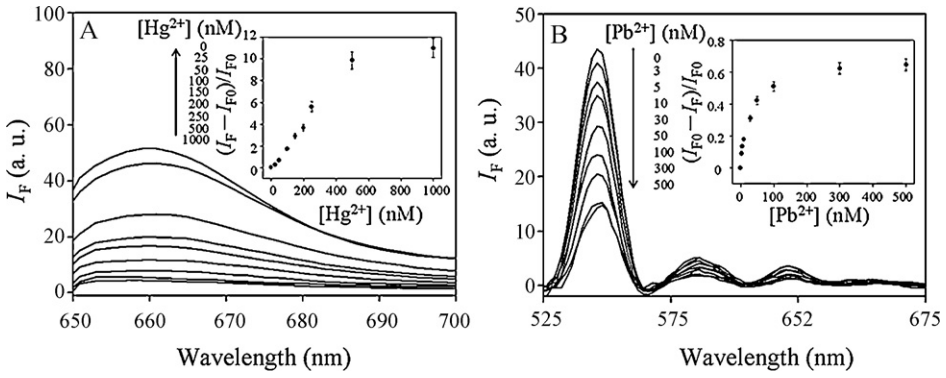

Fig. 5. Fluorescence spectra of solutions containing (A) T_{33} (10 nM) and TOTO-3 (20 nM) after addition of Hg^{2+} ions (0, 25, 50, 100, 150, 200, 250, 500, or 1000 nM) and (B) the mixtures in (A) spiked with T_{33} (1.0 μM), G_{33} (10 nM), and Tb^{3+} (100 nM) after addition of Pb^{2+} ions (0, 3, 5, 10, 30, 50, 100, 300, or 500 nM). *Insets*: Fluorescence ratios plotted with respect to (A) Hg^{2+} and (B) Pb^{2+} ion concentrations. Other conditions were the same as those described in Fig. 1. I_F and I_{F0} represent fluorescence intensities in the presence and absence, respectively, of (A) Hg^{2+} and (B) Hg^{2+} and Pb^{2+} ions.

lower than that of Pb^{2+} ions with G quartet through melting point measurement [38]. As a result, K^+ ions did not cause interference on the detection of Pb^{2+} ions in this study. The presence of higher concentrations (>1.0 μM) of Hg^{2+} ions, however, also led to decreases in the fluorescence of Tb^{3+}, leading to false-positive signals. Thus, at concentrations of 100 nM or greater, Hg^{2+} ions could compete with Tb^{3+} ions for interactions with G_{33}. To overcome this problem, we added T_{33} to the mixture of Hg^{2+} and Pb^{2+} ions. Fig. 4 reveals that the presence of T_{33} (1.0 μM) minimized the interference of Hg^{2+} ions during the determination of Pb^{2+} ions. Indeed, the G_{33}/Tb^{3+} conjugates in the presence of T_{33} (1.0 μM) provided high selectivity toward Pb^{2+} ions over all of the other tested interference ions. The nature of anions in lead compounds also did not play major roles in the detection of Pb^{2+} ions (such as $PbCl_2$, $Pb(NO_3)_2$ and $PbSO_4$).

3.4. Sensitivity and applications

Under the optimal conditions, we investigated the sensitivity of the T_{33}/TOTO-3 conjugates toward Hg^{2+} ions and the G_{33}/Tb^{3+} conjugates toward Pb^{2+} ions. The fluorescence of TOTO-3 increased upon increasing the concentration of Hg^{2+} (Fig. 5A). We obtained a linear response of the expression $(I_F - I_{F0})/I_{F0}$ against the concentration of Hg^{2+} over the range 25.0–500 nM ($R^2 = 0.99$), with the LOD down to 10.0 nM, which is below the maximum level of Hg^{2+} permitted by the U.S. EPA for drinking water. The fluorescence of the G_{33}/Tb^{3+} conjugates decreased upon increasing the concentration of Pb^{2+} ions (Fig. 5B). We obtained a linear response of the expression $(I_{F0} - I_F)/I_{F0}$ against the concentration of Pb^{2+} ions over the range 3.0–50 nM ($R^2 = 0.98$), with the down to 1.0 nM, which is well below the maximum level of Pb^{2+} ions permitted by the U.S. EPA for drinking water. Relative to most other optical detection systems, the G_{33}/Tb^{3+} conjugates displays much better sensitivity toward Pb^{2+} ions [46]. Compared with our previous approach [16,18], this detection system (T_{33}/TOTO-3 and G_{33}/Tb^{3+} conjugates) provides comparable sensitivity for Hg^{2+} ions, but slightly lower (3 times) sensitivity for Pb^{2+} ions. This approach has advantages of low cost (DNA was not labelled with a fluorophore and quencher) and simplicity (adding a masking agent to reduce matrix interference is not required). Relative to ICP-MS-based analysis, our approach provided advantages of low cost, simplicity, and rapidity.

To test the practicality of this present probe, we first analyzed Hg^{2+} and Pb^{2+} ions in the soil sample by a standard addition method. Based on five repeated measurements, we obtained concentrations

Table 1
Fluorescence, colorimetric and electrochemical detection of Hg^{2+} and Pb^{2+} ions.

Method	Probe	Target(s)	LOD[a]	Masking reagent	Real sample	Ref.
Fluorescence	Au nanodots	Hg^{2+}	5.0 nM	2,6-Pyridinedicarboxylic acid	Water sample	[8]
	Rhodamine derivatives	Hg^{2+}	5.0 nM	Not necessary	–	[10]
	FAM-DNA-DABCYL	Hg^{2+}/Pb^{2+}	5.0 nM/300 pM	Phytic acid and a random DNA/NaCN mixture	Soil sample[b], water sample	[16]
	DNA, TOTO-3	Hg^{2+}	3.0 nM	Not necessary	Water sample, battery[c]	[18]
	DNA	Pb^{2+}	20 nM	Not necessary	–	[19]
	FAM-DNAzyme-DABCYL	Pb^{2+}	3.0 nM	Not necessary	–	[22]
	FAM-DNAzyme-DABCYL	Pb^{2+}	10 nM	Not necessary	–	[25]
	DNA, TOTO-3, Tb^{3+}	Hg^{2+}/Pb^{2+}	10 nM/1.0 nM	Not necessary	Soil sample, Water sample	This study
Colorimetric	Au NPs	Hg^{2+}	10 nM	2,6-Pyridinedicarboxylic acid	Water sample, battery[c]	[9]
	DNA, Au NPs	Hg^{2+}	0.6 nM	Not necessary	Water sample	[20]
	DNAzyme, Au NPs	Pb^{2+}	500 nM	Not necessary	–	[23]
	DNA-Au NPs	Hg^{2+}	10 nM	Not necessary	Water sample	[27]
	DNA, Au NPs	Hg^{2+}	250 nM	Not necessary	–	[28]
	DNA-Au NPs	Hg^{2+}	100 nM	Not necessary	–	[30]
	DNA, Au NPs	Hg^{2+}	500 nM	Not necessary	–	[36]
	Alkaline phosphatase	Pb^{2+}	0.1 nM	Not provided	Soil sample	[13]
	Horseradish peroxidase	Hg^{2+}	0.5 pM	Not provided	Water sample	[14]
Electrochemical	DNA–TiO_2 nanotube	Pb^{2+}	3.3 pM	Not necessary	Water sample	[5]
	DNAzyme	Pb^{2+}	300 nM	Not necessary	Soil sample[b]	[7]
	DNA	$Cu^{2+}/Pb^{2+}/Cd^{2+}$	0.4 pM/0.1 nM/1.0 nM	Not necessary	Water sample	[12]

[a] The LOD is defined as the concentration of metal ions at a signal-to-noise ratio of 3. 1.0 nM Hg^{2+} and Pb^{2+} ions are equal to 0.20 and 0.21 μg L^{-1}, respectively.
[b] Acidic digestion of soil samples (0.01 g) was performed according to EPA Method 305B.
[c] The sample preparation of a button-type alkaline manganese battery was according to the standard method published by the National Electrical Manufacturers Association.

of 31 (±1.1) and 5552 (±70) μg/g, respectively (cf. values of 32 and 5532 μg/g provided by NIST). Using a *t*-test (the *t*-test value was 2.776 at a 95% confidence level), the 95% confidence intervals for Hg^{2+} and Pb^{2+} ions were 30–32 and 5465–5639 μg/g, respectively, revealing that no significant differences existed between the values measured using our new approach and the true values. We also obtained linear correlations ($R^2 > 0.98$) between the responses and the concentrations of Hg^{2+} and Pb^{2+} ions spiked into the pond water over the ranges 25–250 and 5.0–50 nM, respectively. The recoveries of these measurements were valued at 95–110%. Neither our probe nor the ICP-MS-based analysis could detect the presence of Hg^{2+} and Pb^{2+} ions in the pond water sample.

4. Conclusions

We have devised a new assay for the sensitive and selective detection of Hg^{2+} and Pb^{2+} ions using T_{33}/TOTO-3 and G_{33}/Tb^{3+} conjugates. The presence of Hg^{2+} ions induced increased fluorescence from the T_{33}/TOTO-3 conjugates through T–Hg^{2+}–T coordination; in contrast, Pb^{2+} ions induced decreased fluorescence from the G_{33}/Tb^{3+} conjugates as a result of competition between the Pb^{2+} and Tb^{3+} ions for interactions with G_{33}. Table 1 compares our present approach with other fluorescence, colorimetric and electrochemical approaches for the detection of Hg^{2+} or/and Pb^{2+} ions with respect to detection limit and specificity. Because of the high specificity of T_{33} toward Hg^{2+} ions and G_{33} toward Pb^{2+} ions, no masking agents were necessary, thereby simplifying the detection process. In addition, because we did not covalently conjugate any dyes to the DNA strands, this approach is relatively inexpensive. We validated its practicality through analyses of soil and water samples. To the best of our knowledge, this system is the first to employ various DNA sequences and different reporters for the detection of both Hg^{2+} and Pb^{2+} ions in the same sample. This simple, rapid, and cost-effective sensing technique holds great practical potential for the detection of heavy metal ions in real samples.

Acknowledgment

This study was supported by the National Science Council of Taiwan under contracts NSC 98-2113-M-002-011-MY3.

Appendix A. Supplementary data

Supplementary data associated with this article can be found, in the online version, at doi:10.1016/j.talanta.2011.01.016.

References

[1] I. Hoyle, R.D. Handy, Aquat. Toxicol. 72 (2005) 147–159.
[2] H.L. Needleman, P.J. Landrigan, Am. J. Public Health 94 (2004) 8–18.
[3] W.J. McShane, R.S. Pappas, V. Wilson-McElprang, D. Paschal, Spectrochim. Acta B 63 (2008) 638–644.
[4] M.G. Minnich, D.C. Miller, P.J. Parsons, Spectrochim. Acta B 63 (2008) 389–395.
[5] M. Liu, G. Zhao, Y. Tang, Z. Yu, Y. Lei, M. Li, Y. Zhang, D. Li, Environ. Sci. Technol. 44 (2010) 4241–4246.
[6] H.A. Zamani, M.R. Ganjali, H. Behmadi, M.A. Behnajady, Mater. Sci. Eng. C 29 (2009) 1535–1539.
[7] Y. Xiao, A.A. Rowe, K.W. Plaxco, J. Am. Chem. Soc. 129 (2007) 262–263.
[8] C.-C. Huang, Z. Yang, K.-H. Lee, H.-T. Chang, Angew. Chem. Int. Ed. 46 (2007) 6824–6828.
[9] C.-C. Huang, H.-T. Chang, Anal. Chem. 78 (2006) 8332–8338.
[10] Y.K. Yang, K.J. Yook, J. Tae, J. Am. Chem. Soc. 127 (2005) 16760–16761.
[11] I. Chang, J. Tulock, J. Liu, W. Kim, D. Cannon Jr., Y. Lu, P. Bohn, J. Sweedler, D. Cropek, Environ. Sci. Technol. 39 (2005) 3756–3761.
[12] S. Babkina, N. Ulakhovich, Anal. Chem. 77 (2005) 5678–5685.
[13] I. Veselova, T. Shekhovtsova, Anal. Chim. Acta 413 (2000) 95–101.
[14] T. Shekhovtsova, S. Chernetskaya, Anal. Lett. 27 (1994) 2883–2898.
[15] D.M. Kong, Y.E. Ma, J.H. Guo, W. Yang, H.X. Shen, Anal. Chem. 81 (2009) 2678–2684.
[16] C.-W. Liu, C.-C. Huang, H.-T. Chang, Anal. Chem. 81 (2009) 2383–2387.
[17] I. Okamoto, K. Iwamoto, Y. Watanabe, Y. Miyake, A. Ono, Angew. Chem. Int. Ed. 48 (2009) 1648–1651.
[18] C.-K. Chiang, C.-C. Huang, C.-W. Liu, H.-T. Chang, Anal. Chem. 80 (2008) 3716–3721.
[19] T. Li, S. Dong, E. Wang, J. Am. Chem. Soc. 132 (2010) 13156–13157.
[20] L. Li, B.X. Li, Y.Y. Qi, Y. Jin, Anal. Bioanal. Chem. 393 (2009) 2051–2057.
[21] Y.L. Li, L. Guo, Z.Y. Zhang, J.J. Tang, J.W. Xie, Sci. China Ser. B 51 (2008) 193–204.
[22] H. Wang, Y.M. Kim, H.P. Liu, Z. Zhu, S. Bamrungsap, W.H. Tan, J. Am. Chem. Soc. 131 (2009) 8221–8226.
[23] H. Wei, B.L. Li, J. Li, S.J. Dong, E.K. Wang, Nanotechnology 19 (2008) 095501–095505.
[24] A.K. Brown, J. Li, C.M.B. Pavot, Y. Lu, Biochemistry-Us 42 (2003) 7152–7161.
[25] J. Li, Y. Lu, J. Am. Chem. Soc. 122 (2000) 10466–10467.
[26] Z.D. Wang, Y. Lu, J. Mater. Chem. 19 (2009) 1788–1798.
[27] J.S. Lee, C.A. Mirkin, Anal. Chem. 80 (2008) 6805–6808.
[28] C.-W. Liu, Y.-T. Hsieh, C.-C. Huang, Z.-H. Lin, H.-T. Chang, Chem. Commun. (2008) 2242–2244.
[29] J.H. Lee, Z.D. Wang, J.W. Liu, Y. Lu, J. Am. Chem. Soc. 130 (2008) 14217–14226.
[30] F. Chai, C. Wang, T. Wang, L. Li, Z. Su, ACS Appl. Mater. Interfaces 2 (2010) 1466–1470.
[31] USEPA SE-846 in Government Printing Office, Washington, DC, 1996.
[32] Y. Tanaka, S. Oda, H. Yamaguchi, Y. Kondo, C. Kojima, A. Ono, J. Am. Chem. Soc. 129 (2007) 244–245.
[33] Y. Miyake, H. Togashi, M. Tashiro, H. Yamaguchi, S. Oda, M. Kudo, Y. Tanaka, Y. Kondo, R. Sawa, T. Fujimoto, T. Machinami, A. Ono, J. Am. Chem. Soc. 128 (2006) 2172–2173.
[34] H. Torigoe, Y. Miyakawa, T. Kozasa, A. Ono, Nucleic Acids Sym. Ser. 51 (2007) 185–186.
[35] H. Torigoe, A. Ono, T. Kozasa, Chem. -Eur. J. 16 (2010) 13218–13225.
[36] X.W. Xu, J. Wang, K. Jiao, X.R. Yang, Biosens. Bioelectron. 24 (2009) 3153–3158.
[37] D. Costa, H.D. Burrows, M.D. Miguel, Langmuir 21 (2005) 10492–10496.
[38] P.K.L. Fu, C. Turro, J. Am. Chem. Soc. 121 (1999) 1–7.
[39] A.L. Feig, M. Panek, W.D. Horrocks, O.C. Uhlenbeck, Chem. Biol. 6 (1999) 801–810.
[40] S.L. Klakamp, W.D. Horrocks, J. Inorg. Biochem. 46 (1992) 175–192.
[41] D.P. Ringer, S. Burchett, D.E. Kizer, Biochemistry-Us 17 (1978) 4818–4825.
[42] F.W. Kotch, J.C. Fettinger, J.T. Davis, Org. Lett. 2 (2000) 3277–3280.
[43] I. Smirnov, R.H. Shafer, J. Mol. Biol. 296 (2000) 1–5.
[44] E. Galezowska, A. Gluszynska, B. Juskowiak, J. Inorg. Biochem. 101 (2007) 678–685.
[45] G. Scatchard, Ann. N. Y. Acad. Sci. 51 (1949) 660–672.
[46] J.W. Liu, Y. Lu, J. Am. Chem. Soc. 125 (2003) 6642–6643.